Research Article | Vol. 26, No. 26 | 24 Dec 2018 | OPTICS EXPRESS 33993
Optics EXPRESS

Averaging-free vector Brillouin optical time domain analyzer assisted by reference probe lightwave

NAN GUO,[1,4] XIANTING ZHANG,[1,4] CHAO JIN,[1] ZHIYONG ZHAO,[1] LIANG WANG,[2,*] HWA-YAW TAM,[3] AND CHAO LU[1]

[1]*Department of Electronic and Information Engineering, Hong Kong Polytechnic University, Kowloon, Hong Kong*
[2]*Department of Electronic Engineering, Chinese University of Hong Kong, Shatin, N.T., Hong Kong*
[3]*Department of Electrical Engineering, Hong Kong Polytechnic University, Kowloon, Hong Kong*
[4]*These authors contribute equally to this work*
**lwang@ee.cuhk.edu.hk*

Abstract: We propose and experimentally demonstrate a vector Brillouin optical time domain analyzer (BOTDA) system, which enables both distributed Brillouin gain spectrum (BGS) and Brillouin phase-shift spectrum (BPS) measurements without trace averaging. The proposed scheme generates and launches a reference light into the fiber under test (FUT), together with the Stokes probe light to indicate the phase noise and distortion in the probe. The commercial integrated coherent receiver at the detection end, using a local oscillator (LO) generated with single sideband (SSB) modulation, on the one hand, improves the signal-to-noise ratio (SNR) to avoid the need of trace averaging for the signal acquisition. On the other hand, by processing and analyzing the receiver outputs at specific intermediate frequencies (IF), the amplitude and phase signals carried by the Stokes probe and the reference light can be resolved at once. In this way, both Brillouin gain and Brillouin phase-shift signals can be obtained simultaneously. By scanning the the Stokes probe light frequency and recording the Brillouin response at each scanning frequency, both distributions of Brillouin gain spectrum and phase-shift spectrum have been acquired. The configuration is approved by experiments carried out over an 18.2 km FUT with the spatial resolution of 2 m.

1. Introduction

Brillouin Optical Time Domain Analyzer (BOTDA) is one of the most popular distributed optical fiber sensing techniques. A lot of research effort has been made to enhance its performance since it was first proposed [1]. BOTDA systems are used to measure the distribution of Brillouin frequency shift (BFS) of a span of fiber under test (FUT), and thus to obtain the distributed temperature and/or strain information. The sensing performance, in terms of spatial resolution, sensing range, and measurand accuracy, is mainly limited by the signal-to-noise ratio (SNR) of the sensor response [2], which is restricted by fiber nonlinearities [3,4], and the non-local effects [5]. In the past few years, coherent detection has been applied to BOTDA systems for SNR enhancement, fast measurement, and as well as Brillouin phase shift detection [6–19]. Brillouin phase shift detection enables dynamic measurement [8,16], and also increases the tolerance to non-local effect [9]. Moreover, Brillouin phase shift detection has shown similar BFS estimation performance [20,21]. As a result of this, the Brillouin gain and phase shift can be combined together to reduce the BFS uncertainty by using support vector machine (SVM) method [17] or complex Brillouin spectrum (CBS) fitting [18].

Recently, we reported a coherent BOTDA system without trace averaging [19]. In most other coherent detection schemes, a local oscillator (LO) lightwave is often generated together with the probe and injected into the fiber under test (FUT) at the same time, where

#351219 https://doi.org/10.1364/OE.26.033993
Journal © 2018 Received 6 Nov 2018; revised 6 Dec 2018; accepted 6 Dec 2018; published 13 Dec 2018

Optics EXPRESS

the power of LO is limited due to the fiber nonlinearities. The local oscillator (LO) in the reported scheme is generated by single sideband (SSB) modulation, and then injected into the coherent receiver directly without propagating in the FUT. By using this scheme, it increases the SNR of the Brillouin response significantly and avoids the need of trace averaging. In order to reduce the polarization dependent fluctuation, a pair of pump pulses in orthogonal polarization states are employed to stimulate two orthogonal Brillouin responses in a row. However, as the probe and the LO are generated and transmitted separately, the Brillouin response is affected by laser phase noise and interferometry phase distortion, making the detection of the Brillouin phase shift impossible.

In this paper, we propose an improved scheme to realize an averaging-free vector BOTDA system, which enables both distributed Brillouin gain spectrum (BGS) and Brillouin phase-shift spectrum (BPS) measurements. A reference light is generated and launched into the FUT together with the Stokes probe light to ensure that they are phase matched to each other. The system employs the same setup as the one used in [19] for the generation of LO and the heterodyne coherent detection, enhancing the SNR intensive enough to acquire the signal in real-time without any trace averaging. In addition, it allows to resolve the amplitude and phase signals carried by the Stokes probe and the reference light from the corresponding intermediate frequencies (IF). The Brillouin gain signals can be resolved from the amplitude of the Stokes probe, while the distorted Brillouin phase signals can be recovered by processing and analyzing the phase of the Stokes probe and reference light. Because the chromatic dispersion (CD) induced by the fiber transmission is a constant value, the phase signal shall not contain the CD component after normalization for Stokes probe light at a given scanning frequency, which makes the scheme not affected by the CD of the FUT. By scanning the frequency of the Stokes probe light and recording the Brillouin response at each scanning frequency, distributions of BGS and BPS are obtained simultaneously in the experimental demonstrations over an 18.3 km FUT with the spatial resolution of 2 m. The BFS uncertainties obtained from the BGS and BPS are 1.5604 and 1.7721 MHz, respectively.

2. Principle

A BOTDA system injects a pulsed pump lightwave and a counter-propagating continuous-wave (CW) probe lightwave into the FUT. The frequency offset between the two lightwaves $\Delta\nu$ is set close to the BFS value ν_B of the FUT, so that stimulated Brillouin scattering (SBS) effect is induced. When the pulse width of the pump lightwave $\Delta\tau$ is longer than the phonon lifetime, the interaction can be analyzed under steady state assumption. And the SBS effect on the probe light can be described by a complex transfer function written as

$$H(t,\Delta\nu)=\exp\left(\frac{g_{B0}(z)P_{P0}\exp(-\alpha z)v_g\Delta\tau}{4A_{eff}}\frac{1}{1+j\left[\Delta\nu-\nu_B(z)\right]/\left[\Delta\nu_B(z)/2\right]}\right)\Bigg|_{z=v_g t/2}, \quad (1)$$

where P_{P0} is the original peak power of the pulsed pump, g_{B0} is the local Brillouin gain coefficient, α is the fiber attenuation coefficient, v_g is group velocity of light in the fiber, A_{eff} is the fiber effective area, ν_B is the local BFS of the fiber, and $\Delta\nu_B$ denotes the Brillouin linewidth. The equation indicates that the effect modifies both amplitude and phase of the probe light, originating from the real and imaginary parts respectively. The normalized Brillouin gain and phase shift spectrum profile at each location point shall expressed as

$$\begin{aligned} g_{B,N}&=\frac{1}{1+\left[(\Delta\nu-\nu_B)/(\Delta\nu_B/2)\right]^2}, \\ \varphi_{B,N}&=\frac{-(\Delta\nu-\nu_B)/(\Delta\nu_B/2)}{1+\left[(\Delta\nu-\nu_B)/(\Delta\nu_B/2)\right]^2}. \end{aligned} \quad (2)$$

Optics EXPRESS

Conventional BOTDA systems usually generate the Stokes probe lightwave by tuning the optical carrier frequency down-shifted by Δv via a clock synthesizer, and then record the intensity of the probe. By scanning the clock synthesizer frequency output f_S and recording the Stokes probe intensity evolution at each scanning frequency, the distribution of Brillouin gain spectrum (BGS) can be reconstructed. Because the BFS value at each location is affected by the ambient temperature or the applied strain, distributed sensing can be realized by extracting the center frequency of the reconstructed BGS distribution.

In order to detect both Brillouin gain and phase shift signals, a vector BOTDA without trace averaging is proposed by introducing a reference probe lightwave and utilizing the heterodyne coherent detection. As shown in Fig. 1(a), the LO is generated by the SSB modulation from the same laser source of the BOTDA system with frequency downshifted by f_{LO}. The probe light consists of the Stokes and reference light, generated by double sideband (DSB) modulation simultaneously, which are upshifted and downshifted by respectively f_S and f_R from the laser source as the Stokes and reference probe lightwaves. If only the lower sideband is considered, the received probe wave optical field for Stokes frequency of f_s is given by

$$\begin{aligned} E(t,f_s) &= E_S(t,f_s) + E_R(t) \\ &= \sqrt{P_{S0}\exp(-\alpha L)}\exp\left\{-j\left[2\pi(v_0 - f_S)t + \varphi_S(f_S) + \varphi_N\right]\right\} H(t,f_S) \\ &+ \sqrt{P_{R0}\exp(-\alpha L)}\exp\left\{-j\left[2\pi(v_0 - f_R)t + \varphi_R(f_R) + \varphi_N\right]\right\} \end{aligned} \quad , \qquad (3)$$

where P_{S0}, P_{R0} are the original powers of the Stokes and reference probe, L is the fiber length, v_0 is the optical frequency of the laser source, φ_S and φ_R are respectively the phase shifts of the lower sideband of the Stokes and reference probe lightwaves caused by fiber link transmission. As the laser phase noise and the interferometry phase distortion affect the Stokes probe and the reference probe by the same amount at any specific point in time, φ_N in Eq. (3) represents the optical phase noise between the LO and the Stokes probe or the reference probe.

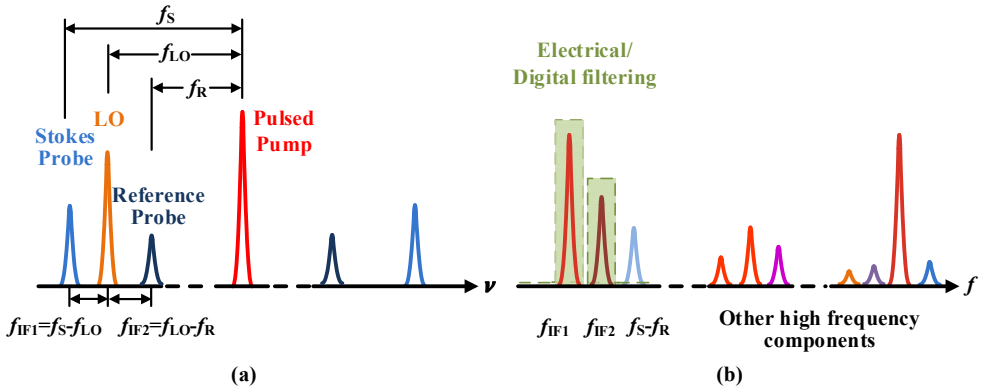

Fig. 1. (a) The frequency alignment of the pulsed pump, the Stokes probe, reference probe and LO in the proposed vector BOTDA; (b) the frequency components at the output of coherent receiver before electrical filtering.

At the detection end, the probe and the LO lightwaves in Fig. 1(a) beat with each other, and the coherent receiver generates the electrical output signals with frequency components as shown in Fig. 1(b). By using electrical low-pass filtering and subsequent digital filtering, the frequency components at $f_{IF1} = f_S - f_{LO}$ and $f_{IF2} = f_R - f_{LO}$, which are the beating signals between the lower sideband of the probe and the LO lightwaves, can be accurately and well

Optics EXPRESS

collected. The detected signal after electrical filtering at each scanning frequency can be expressed as

$$\begin{aligned} I(t,f_S)&=I_S(t,f_S)+I_R(t)\\ &=\frac{R}{2}\sqrt{P_{S0}P_{LO}\exp(-\alpha L)}\,H(t)\big|_{f_S}\exp\left[j\left(2\pi f_{IF1}t-\varphi_{LO}+\varphi_S(f_S)+\varphi_N\right)\right]\\ &\quad+\frac{R}{2}\sqrt{P_{R0}P_{LO}\exp(-\alpha L)}\exp\left[j\left(-2\pi f_{IF2}t-\varphi_{LO}+\varphi_R(f_R)+\varphi_N\right)\right]+\text{c.c}\\ &=\frac{R}{2}\sqrt{P_{LO}P_{S0}\exp(-\alpha L)}\left(1+g_B(t,f_S)\right)\exp\left[j\left(2\pi f_{IF1}t-\varphi_{LO}+\varphi_S(f_S)+\varphi_B(t,f_S)+\varphi_N\right)\right]\\ &\quad+\frac{R}{2}\sqrt{P_{LO}P_{R0}\exp(-\alpha L)}\exp\left[j\left(-2\pi f_{IF2}t-\varphi_{LO}+\varphi_R(f_R)+\varphi_N\right)\right]+\text{c.c} \end{aligned}, \tag{4}$$

where R is the responsivity of the receiver, P_{LO} is the power of the LO light. As a commercial phase- and polarization-diversity coherent receiver is used for coherent detection, the in-phase and quadrature-phase components of the signals in Eq. (1) in both X, Y polarizations are received simultaneously via the four outputs of the receiver, represented as I_{XI}, I_{XQ}, I_{YI}, and I_{YQ}. Two complex signals are constructed as

$$S_X = I_{XI} + jI_{XQ}\,,\quad S_Y = I_{YI} + jI_{YQ}\,, \tag{5}$$

and then processed using the designed digital signal processing (DSP) algorithms. They are filtered by two respective digital bandpass filters designed with a center frequency at f_{IF1} and f_{IF2} to obtain four sets of complex signals S_{SX}, S_{SY}, S_{RX}, and S_{RY}, namely the Stokes and reference signals of X and Y polarizations.

The amplitude and phase signals of the Stokes probe lightwave can be obtained as

$$\begin{aligned} A_S(t,f_S)&=\sqrt{|S_{SX}|^2+|S_{SY}|^2}\\ &=\frac{R}{2}\sqrt{P_{S0}P_{LO}\exp(-\alpha L)}\left(1+g_B(t,f_S)\right)\\ \Phi_S(t,f_S)&=\left[\arg(S_{SX})+\arg(S_{SY})\right]/2-2\pi f_{IF1}t\\ &=-\varphi_{LO}+\varphi_S(f_S)+\varphi_B(t,f_S)+\varphi_N \end{aligned}\,,\ . \tag{6}$$

The Brillouin gain signal can then be obtained by removing the direct-current (DC) part of the amplitude signal

$$G_B(t,f_S)=g_B(t,f_S)R\sqrt{P_{S0}P_{LO}\exp(-\alpha L)/2}\,. \tag{7}$$

But the Brillouin phase shift signal carried by the Stokes probe lightwave is impossible to be resolved only from analyzing its phase signal, as it is distorted by the phase noise φ_N. However, the phase information of the reference probe could be easily acquired as

$$\begin{aligned} \Phi_R(t,f_R)&=\left[\arg(S_{RX})+\arg(S_{RY})\right]/2+2\pi f_{IF2}t\\ &=-\varphi_{LO}+\varphi_R(f_R)+\varphi_N \end{aligned}\,, \tag{8}$$

By making use of this, the Brillouin phase shift signal can be resolved by calculating the phase difference between the two probe lightwaves as shown as

$$\varphi_B(t,f_s)=\Phi_S(t,f_S)-\Phi_R(t,f_R)-\left[\varphi_S(f_S)-\varphi_R(f_R)\right], \tag{9}$$

Optics EXPRESS

which is unaffected by the laser phase noise and interferometry phase distortion during the transmission. The only unknown values of φ_S and φ_R in Eq. (9) vary with the Stokes and reference probe frequency respectively due to the CD effects. However, the amount of phase shift induced by them remains constant with or without Brillouin interaction for given f_S and f_R. As a result, after removing the DC component from the calculated result of Eq. (9) for each Stokes frequency, only the estimated Brillouin phase shift signal is maintained.

In order to suppress the polarization dependent noise in the proposed coherent scheme and to maintain the real-time signal acquisition, we adopt the polarization diversity structure with the use of a polarization switch [22]. Adjacent pump pulses are made orthogonal in polarization to each other by using a polarization switch driven by level signals that are synchronized with the pump pulse generation at the same repetition rate, as shown in Fig. 2. As a result of this, the polarization orthogonal Brillouin responses can be combined to suppress the polarization dependent fluctuations in the recovered Brillouin gain and Brillouin phase shift traces.

Fig. 2. The configuration of orthogonal pump pulse sequence at each scanning frequency to suppress polarization dependent fluctuation.

3. Experiment setup

Figure 3 shows the experiment setup of the proposed averaging-free vector BOTDA system. The output light of a 1550 nm laser is split into three branches by 20/80 and 50/50 couplers, respectively.

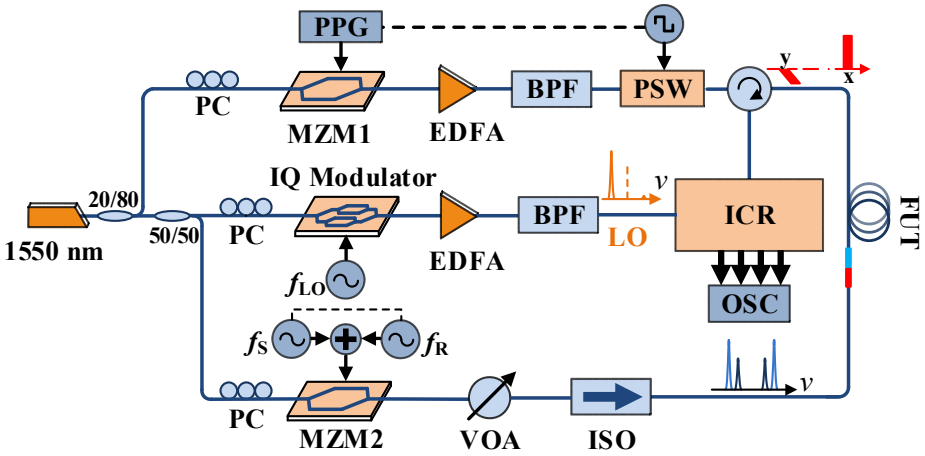

Fig. 3. Experiment setup of the coherent-detection-assisted BOTDA without trace averaging. PC, polarization controller; EDFA, Erbium-doped fiber amplifier; BPF, band pass filter; MZM, Mach-Zehnder Modulator; PPG, pulse pattern generator; PSW, polarization switch; VOA, variable optical attenuator; ISO, isolator; OSC, Oscilloscope; FUT, fiber under test.

In the upper branch, a high-extinction-ratio Mach-Zehnder modulator (MZM1, 40 dB extinction ratio) and a pulse pattern generator (PPG) are employed to generate pump pulses with pulse width of 20 ns, corresponding to spatial resolution of 2 m. The erbium-doped fiber amplifier (EDFA) in the branch boosts the peak power of the pulses to about 21 dBm, and a bandpass filter with the bandwidth of 1 nm is used to reduce the amplified spontaneous

Optics EXPRESS

emission (ASE) noise from the EDFA. A polarization switch (PSW), driven by a function generator synchronized with the pump pulses, enables two sequential Brillouin responses orthogonal to each other to suppress the polarization dependent fluctuations of Brillouin signals. Then the pump pulses are delivered to the FUT through a circulator. Operated in single-sideband (SSB) modulation mode, the IQ modulator in the middle branch together with a radio frequency (RF) synthesizer with fixed output frequency of 10 GHz are used to generate a lightwave as the local oscillator (LO) for coherent detection. During the generation of the LO lightwave, the carrier and the upper sideband are successfully suppressed by up to 30 dB and 40 dB respectively. An EDFA is used to boost the LO power to around 10 dBm, and a BPF is used to suppress ASE noise.

On the other hand, the lower branch produces dual double-sideband probe lightwaves by MZM2 and two synchronized radio frequency (RF) synthesizers. The tunable RF synthesizer provides the scanning frequencies f_S for the Stokes probe from 10.75 to 10.93 GHz with a scanning step of 1 MHz to reconstruct the distributed BGS and BPS, and the other fixed at 9 GHz is employed as f_R for the generation of the reference light. The power of the lower sideband of the Stokes probe and reference light are about −8 dBm and −17 dBm. Thus, the IF signals carrying Brillouin gain and phase shift vary from 750 to 930 MHz, while the ones carrying the reference phase is a constant frequency of 1 GHz. A variable optical attenuator (VOA) is inserted to control the power of each sideband, and an isolator is followed to block the counter-propagating pump lightwave.

The probe lightwaves after propagating in the fiber under test (FUT) and the LO are then injected into the commercial integrated coherent receiver (ICR, Fujitsu FIM24704). The in-phase and quadrature-phase signals of the two orthogonal polarizations are collected at a sampling rate of 5 GSample/s in real-time manner by the four channels of an oscilloscope (OSC) with a low pass filter (DC-1.3GHz) at each channel employed to block the unwanted high-frequency components. During the DSP progress, the bandwidth of each digital bandpass filter is related to the signal bandwidths carried by the IF. In our condition, as the IF at f_{IF1} carries the Brillouin response signals, the filter bandwidth shall be limited by the spatial resolution of the system. While the one at f_{IF2} only carries the phase reference, the filter bandwidth can be set much narrower compared to the former one. Therefore, a digital bandpass filter with bandwidth of 120 MHz is employed to extract the signal at f_{IF1} in the frequency domain. While another one with bandwidth of 2 MHz is employed to obtain the signal at f_{IF2}.

4. Experimental results

In this experimental demonstration, the FUT is composed with an 18 km single-mode fiber (FUT I) and a 226 m single-mode fiber (FUT II). By taking use of conventional BOTDA setup, the average BFS of FUT I and II are calibrated as ~10.83 and 10.86 GHz, respectively, placed in an oven and kept under 25 °C.

Based on the proposed principle and experiment setup given in last two sections, the Brillouin phase shift signal can be successfully resolved with the assistance of the reference probe lightwave. For instance, at the scanning frequency of 10.857 GHz, the resolved phase signals of the Stokes and reference probe lightwaves are totally distorted by the phase noise between the probe and the LO lightwaves as illustrated in Fig. 4(a). The initial values of the two signal traces are also different due to the CD effects on the two probe lightwaves. However, by simply subtracting the two signals and removing its DC part, the Brillouin phase shift signal at this scanning frequency is obtained as shown in Fig. 4(b).

Optics EXPRESS

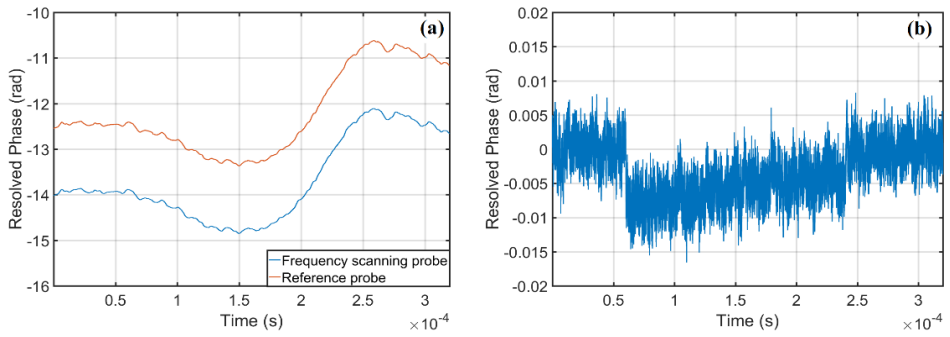

Fig. 4. (a) Resolved phase of the Stokes and reference probe lightwave, (b) resolved Brillouin phase shift distribution at scanning frequency of 10.857 GHz.

In Fig. 5(a) and 5(b), the reconstructed BGS and BPS distributions along the whole FUT are illustrated. Figure 5(c) and 5(d) show the top view of the two distributions along the last ~300 m fiber, respectively, where in each figure the distribution of FUT II is clearly distinguished from the previous FUT I.

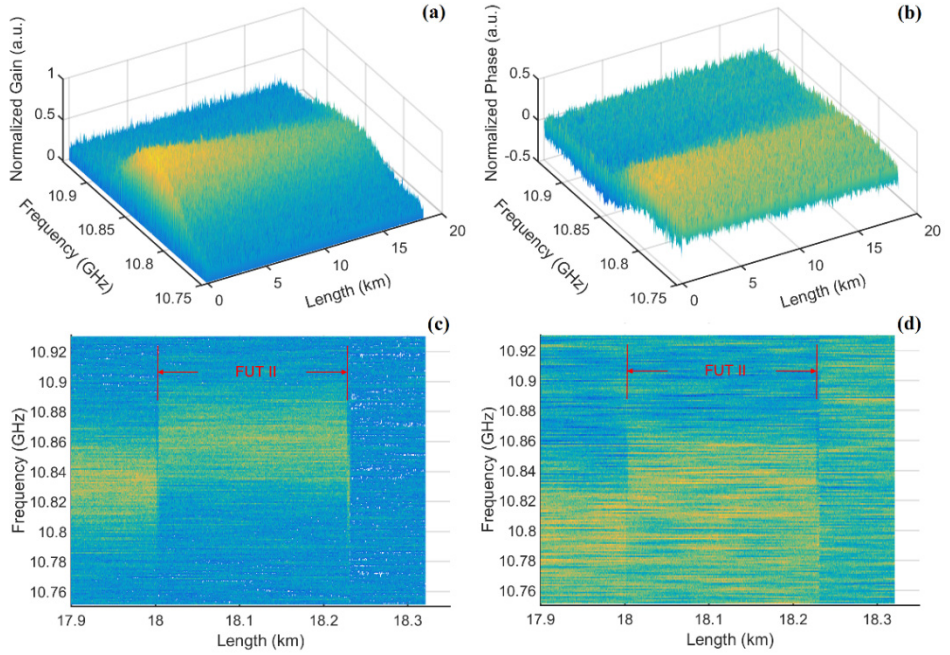

Fig. 5. Reconstructed (a) BGS and (b) BPS distribution along the whole FUT; (c) BGS and (d) BPS distribution along the last ~300 m (top view).

With the help of least square curve fitting based on the measured noisy BGS and BPS curves with the ideal normalized Brillouin gain and phase shift profiles given in Eq. (2), the restored BGS and BPS curves shall give the resolved local BFS values. As shown in Fig. 6, the local BGS and BPS profiles at the point of 18.05 km located in FUT II section are restored from the measured noisy curves. According to the definitions of SNR given in [21], the average SNR values of Brillouin gain and phase-shift spectra in Fig. 6 are calculated to be 6.04 dB and 4.63 dB, respectively.

Optics EXPRESS

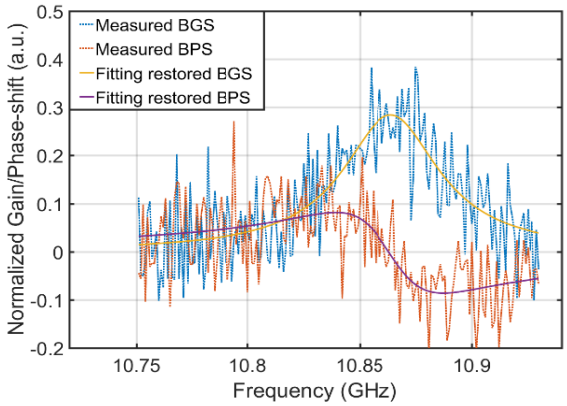

Fig. 6. At location point of 18.05 km: measured BGS, measured BPS, restored BGS and resolved BPS by least square curve fitting.

In Fig. 7, the BFS distributions obtained by using least square curve fitting method have been illustrated. As shown in Fig. 7(a), the BFS uncertainty for each distribution, which is defined as the standard deviation of the restored BFS values along the last 226m fiber (FUT II), is calculated to be 1.5604 and 1.7721 MHz, respectively. It can also be seen from Fig. 7(b) that both BGS and BPS measurements realize the spatial resolution of 2 m, from the length of the transition section between FUT I and II.

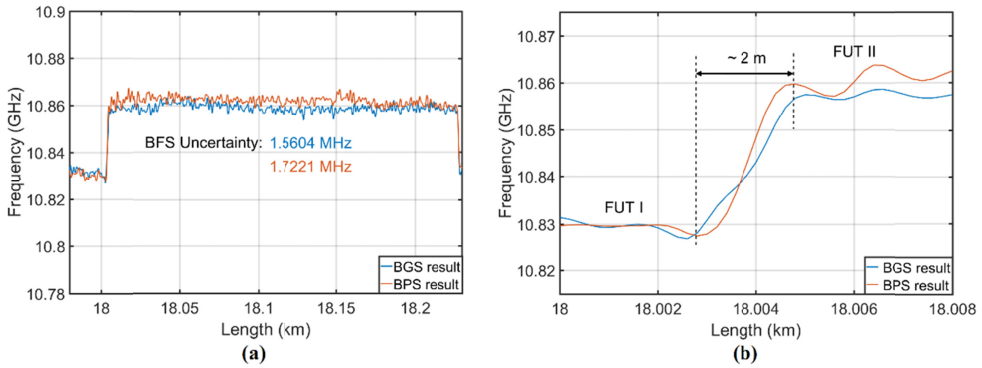

Fig. 7. Measured BFS distributions (a) around the last ~250 m fiber, and (b) around the location with temperature transition.

5. Conclusion

An averaging-free vector BOTDA scheme is proposed to enable both measurements of the BGS and BPS distributions along the FUT. In the scheme, the Stokes probe light carries two orthogonal Brillouin responses in a row to minimize the polarization fluctuation of the SBS interaction. At the same time, a reference probe lightwave is generated and transmitted together with the Stokes probe lightwave to indicate the phase noise. At the detection end, the Stokes and reference probe lightwaves are injected into a commercial integrated coherent receiver with the LO generated by the SSB modulation. The output IF signals of the receiver are then collected by a real-time oscilloscope without any trace averaging. The Brillouin gain and phase-shift signals can be resolved from the SNR enhanced IF signals by using DSP algorithms. As the phase shift induced by the CD effect is constant value at each scanning frequency, it will not be involved in the detected phase signals after normalization during the processing. By using the proposed principle and experiment setup, the distributions of BGS and BPS are obtained simultaneously over an 18.2 km FUT with the spatial resolution of 2 m.

Optics EXPRESS

The BFS uncertainties obtained from the BGS and BPS are 1.5604 and 1.7721 MHz, respectively.

Funding

National Natural Science Foundation of China (NSFC: 61435006); the Research Grants Council (RGC) of Hong Kong, General Research Fund (GRF: PolyU 152658/16E, 152168/17E); The Hong Kong Polytechnic University (1-YW0S, 1-YW3G, 1-ZVFL).

References

1. T. Horiguchi and M. Tateda, "Optical-fiber-attenuation investigation using stimulated Brillouin scattering between a pulse and a continuous wave," Opt. Lett. **14**(8), 408–410 (1989).
2. M. A. Soto and L. Thévenaz, "Modeling and evaluating the performance of Brillouin distributed optical fiber sensors," Opt. Express **21**(25), 31347–31366 (2013).
3. L. Thévenaz, S. F. Mafang, and J. Lin, "Effect of pulse depletion in a Brillouin optical time-domain analysis system," Opt. Express **21**(12), 14017–14035 (2013).
4. M. Alem, M. A. Soto, and L. Thévenaz, "Modelling the depletion length induced by modulation instability in distributed optical fibre sensors," in 23rd International Conference on Optical Fibre Sensors, (Proc. SPIE, 2014), pp. 91575–91575.
5. A. Dominguez-Lopez, X. Angulo-Vinuesa, A. Lopez-Gil, S. Martin-Lopez, and M. Gonzalez-Herraez, "Non-local effects in dual-probe-sideband Brillouin optical time domain analysis," Opt. Express **23**(8), 10341–10352 (2015).
6. M. Dossou, D. Bacquet, and P. Szriftgiser, "Vector Brillouin optical time-domain analyzer for high-order acoustic modes," Opt. Lett. **35**(22), 3850–3852 (2010).
7. A. Zornoza, M. Sagues, and A. Loayssa, "Self-Heterodyne Detection for SNR Improvement and Distributed Phase-Shift Measurements in BOTDA," J. Lightwave Technol. **30**(8), 1066–1072 (2012).
8. J. Urricelqui, A. Zornoza, M. Sagues, and A. Loayssa, "Dynamic BOTDA measurements based on Brillouin phase-shift and RF demodulation," Opt. Express **20**(24), 26942–26949 (2012).
9. J. Urricelqui, M. Sagues, and A. Loayssa, "BOTDA measurements tolerant to non-local effects by using a phase-modulated probe wave and RF demodulation," Opt. Express **21**(14), 17186–17194 (2013).
10. X. Tu, Q. Sun, W. Chen, M. Chen, and Z. Meng, "Vector Brillouin Optical Time-Domain Analysis with Heterodyne Detection and IQ Demodulation Algorithm," IEEE Photonics J. **6**(2), 1–8 (2014).
11. Z. Li, L. Yan, L. Shao, W. Pan, and B. Luo, "Coherent BOTDA sensor with intensity modulated local light and IQ demodulation," Opt. Express **23**(12), 16407–16415 (2015).
12. Z. Li, L. Yan, L. Shao, W. Pan, B. Luo, J. Liang, and H. He, "Coherent BOTDA Sensor with Single-Sideband Modulated Probe Light," IEEE Photonics J. **8**(1), 1–8 (2016).
13. Z. Li, L. Yan, L. Shao, W. Pan, B. Luo, J. Liang, H. He, and Y. Zhang, "Precise Brillouin gain and phase spectra measurements in coherent BOTDA sensor with phase fluctuation cancellation," Opt. Express **24**(5), 4824–4833 (2016).
14. L. Wang, N. Guo, C. Jin, K. Zhong, X. Zhou, J. Yuan, Z. Kang, B. Zhou, C. Yu, H. Y. Tam, and C. Lu, "Coherent BOTDA Using Phase- and Polarization-Diversity Heterodyne Detection and Embedded Digital Signal Processing," IEEE Sens. J. **17**(12), 3728–3734 (2017).
15. J. Fang, P. Xu, Y. Dong, and W. Shieh, "Single-shot distributed Brillouin optical time domain analyzer," Opt. Express **25**(13), 15188–15198 (2017).
16. C. Jin, L. Wang, Y. Chen, N. Guo, W. Chung, H. Au, Z. Li, H. Y. Tam, and C. Lu, "Single-measurement digital optical frequency comb based phase-detection Brillouin optical time domain analyzer," Opt. Express **25**(8), 9213–9224 (2017).
17. H. Wu, L. Wang, N. Guo, C. Shu, and C. Lu, "Support vector machine assisted BOTDA utilizing combined Brillouin gain and phase information for enhanced sensing accuracy," Opt. Express **25**(25), 31210–31220 (2017).
18. J. Fang, M. Sun, D. Che, M. Myers, H. Bao, C. Prohasky, and W. Shieh, "Complex Brillouin optical time domain analysis," IEEE J. Lightwave Technol., PP(99), 1–10, DOI: 10.1109/JLT.2018.2792440 (2018).
19. N. Guo, L. Wang, H. Wu, C. Jin, H. Y. Tam, and C. Lu, "Enhanced Coherent BOTDA System without Trace Averaging," J. Lightwave Technol. **36**(4), 871–878 (2018).
20. A. Lopez-Gil, X. Angulo-Vinuesa, M. A. Soto, A. Dominguez-Lopez, S. Martin-Lopez, L. Thévenaz, and M. Gonzalez-Herraez, "Gain vs phase in BOTDA setups," in Sixth European Workshop on Optical Fibre Sensors, (Proc. SPIE, 2016), paper 991631.
21. A. Lopez-Gil, M. A. Soto, X. Angulo-Vinuesa, A. Dominguez-Lopez, S. Martin-Lopez, L. Thévenaz, and M. Gonzalez-Herraez, "Evaluation of the accuracy of BOTDA systems based on the phase spectral response," Opt. Express **24**(15), 17200–17214 (2016).
22. K. Hotate, K. Abe, and K. Y. Song, "Suppression of Signal Fluctuation in Brillouin Optical Correlation Domain Analysis System Using Polarization Diversity Scheme," IEEE Photonics Technol. Lett. **18**(24), 2653–2655 (2006).